Int. J. Heat Mass Transfer. Vol. 21, pp. 1299–1308
Pergamon Press Ltd. 1978. Printed in Great Britain

MASS TRANSFER FOR TURBULENT FLOW IN AN ANNULUS WITH NON-AXISYMMETRIC BOUNDARY CONDITIONS

D. P. ROBINSON* and V. WALKER
University of Bradford, Bradford, West Yorkshire, England

(*Received* 30 *August* 1977 *and in revised form* 27 *February* 1978)

Abstract—The principal objective of this investigation was to determine the magnitude of circumferential diffusion arising from non-axisymmetric boundary conditions in symmetrical passages free from secondary flows. A concentric annulus was chosen because, with its relatively long circumferential diffusion path, it provides a more sensitive test of diffusion models than does a circular tube; a mass-transfer method was preferred because it avoids problems of heat loss and heat conduction in the tube walls. Nitrous oxide was introduced into the air stream through porous regions in the outer wall and the measured downstream concentration distributions were compared with theoretical solutions. Preliminary measurements were made to verify the representation of the velocity profile and, using an axisymmetric nitrous oxide source, the formulation for the radial eddy diffusivity of mass. Finally, measured concentration distributions arising from non-axisymmetric injection were compared with predictions based upon several alternative formulations for the diffusivity ratio, $\varepsilon_{M,\phi}/\varepsilon_{M,r}$. The isotropic assumption underestimates the magnitude of circumferential diffusion. An excellent fit to all the experimental data was obtained with a model due to Ramm and Johannsen in which the ratio $\varepsilon_{M,\phi}/\varepsilon_{M,r}$ varies with radial position and increases markedly as the walls are approached.

NOMENCLATURE

a, radius of a circular tube;
c, concentration of diffusing substance;
d_e, equivalent diameter;
c_m, mixed mean concentration;
D, diffusivity of mass;
K, constant in von Karman's similarity hypothesis;
n^2, coefficient in Deissler's expression (equation 4);
r, radial coordinate;
r_m, radius of maximum velocity;
R, non-dimensional radius defined in text;
R_{mn}, eigenfunction;
s, radius ratio, r_2/r_1;
u, axial velocity;
u^*, friction velocity:
u^+, non-dimensional axial velocity, u/u^*;
v', RMS average of instantaneous velocity in radial direction;
w', RMS average of instantaneous velocity in circumferential direction;
x, axial coordinate;
x^+, non-dimensional axial coordinate, $\dfrac{x}{2(r_2-r_1)ReSc}$;
y, normal distance from wall;
$\hat{y}$, normal distance from wall to position of maximum velocity;
y^+, non-dimensional distance from wall, yu^*/v;
A_n, B_n, C_m, K_{mn}, coefficients in series;
β_{mn}, γ_n, eigenvalues;
ε, eddy diffusivity;
θ, non-dimensional concentration, c/c_m;
ν, kinematic viscosity;
ρ, non-dimensional radial coordinate, $r/2(r_2-r_1)$;
τ, shear stress;
ϕ, angular coordinate;
Re, Reynolds number based upon equivalent diameter;
Re', Reynolds number for a tube based upon centre-line velocity (quoted by Laufer);
Pr, Prandtl number;
Sc, Schmidt number;
Sc_t, turbulent Schmidt number.

Suffixes

h, heat;
i, initial;
m, momentum;
M, mass;
r, in radial direction;
ϕ, in circumferential direction;
1, inner surface of annulus, or inner region;
2, outer surface of annulus, or outer region.

INTRODUCTION

THIS investigation formed part of a group of studies on three-dimensional turbulent heat and mass transfer in passages of various shapes. It was particularly designed as a study of transverse or circumferential diffusion arising from non-axisymmetric boundary

*Now at United Kingdom Atomic Energy Authority, Dorchester.

conditions in a symmetrical passage free from secondary flows, namely a parallel, concentric annulus.

Reynolds [1] presented a solution for hydrodynamically and thermally fully-developed flow in a circular tube with a prescribed circumferentially varying heat flux at the inner surface. An eddy diffusivity of momentum distribution due to Cess [2] was used along with Jenkins' [3] expression for the turbulent Prandtl number. It was assumed that $\varepsilon_{h\phi} = \varepsilon_{hr}$. Reynolds [4] extended his analysis to the case in which the heat source strength in the tube wall is specified as a function of ϕ, and the solution included the redistribution of heat by conduction in the tube wall. Sparrow and Lin [5] independently obtained a solution to the problem treated in Reynolds' first paper, applicable to a boundary condition of specified circumferential variation of heat flux or temperature at the inner surface of the tube. Again it was assumed that $\varepsilon_{h\phi} = \varepsilon_{hr}$, and the eddy diffusivity distribution used had a zero value on the centre-line, which is a weakness in problems with non-axisymmetric boundary conditions and significant temperature gradients in the centre of the tube. Sutherland and Kays [6] extended the theoretical treatment to concentric annular passages for circumferentially varying heat fluxes at one or both surfaces with allowance for heat conduction in the walls. Again $\varepsilon_{h\phi}$ and ε_{hr} were equated. The relative severity of the circumferential temperature variations increased rapidly as r_2/r_1 approached 1.0, arising from the long circumferential diffusion path.

In order to test the theoretical predictions for circular tubes Black and Sparrow [7] carried out experiments with air flowing through an electrical resistance heated tube with a circumferentially varying wall thickness. The inner surface heat flux distribution was deduced from the heat source distribution and the measured temperatures on the outer tube surface. Circumferential redistribution by conduction in the tube wall was very substantial. Measurements of the air temperature distribution over the tube cross-section were made in the fully-developed region. It was concluded that $\varepsilon_{h\phi}/\varepsilon_{hr}$ is approximately unity over most of the flow cross-section but is substantially greater than unity, perhaps about ten, in the immediate neighbourhood of the wall. Despite the care taken during the investigation there must be some doubt whether the data are sufficiently accurate to substantiate the conclusions. Reference has already been made to very substantial circumferential redistribution of the heat flux by conduction in the tube wall; moreover Rapier [8] has drawn attention to the neglect of the temperature dependence of the electrical resistivity of the tube material, and of circumferential conduction in the thermal insulation surrounding the tube.

To avoid the complication of conduction in the tube wall, Quarmby and Anand [9] employed a mass-transfer technique. Dilute concentrations of nitrous oxide in the air flow through the tube were produced (a) by a diametral line source and (b) by a discontinuous ring source in the tube wall, and the downstream decay of the distributions was investigated. (A preceding investigation by the same workers [10] with axisymmetric nitrous oxide distributions had established the velocity profile and the radial variations of ε_{mr} and ε_{Mr}.) The measured distributions of nitrous oxide were compared with solutions of the diffusion equation with $\varepsilon_{M\phi}$ and ε_{Mr} taken to be equal. Excellent agreement was reported between calculated and observed concentration distributions. In view of certain errors and inconsistencies in the two papers [9] and [10] and in the thesis of Anand [11], and which are summarised in Appendix 1, the excellent agreement between theory and experiment must be regarded as somewhat fortuitous. Moreover Quarmby and Anand recognised that the strongest conclusion to be drawn from their measurements was that they failed to disprove the hypothesis that $\varepsilon_{M\phi}$ and ε_{Mr} are equal. Further calculations reported by Quarmby [13] reinforced the point that the fit between other predictions and the measured concentration profiles [9] would have been equally satisfactory.

Quarmby and Quirk [14] reported further experiments involving the diffusion of heat or mass (nitrous oxide) from sources in the wall of a circular pipe into an air stream. Eddy diffusivity data were deduced by the substitution of temperature or concentration gradients, derived from distribution measurements, into the differential equation. The results exhibited substantial scatter despite great care with the experimental and numerical methods. Nevertheless it could be concluded that (a) heat- and mass-transfer results were consistent, (b) $\varepsilon_{M\phi}/\varepsilon_{Mr}$ is unity over the greater part of the cross-section but rises steeply towards the wall to attain a value of at least ten.

Gärtner, Johannsen and Ramm [15] developed a further theoretical solution for the temperature distribution in a circular pipe with non-axisymmetric boundary conditions. {In this paper also there is an error in the boundary condition at the axis of the tube [equation (9b) of the paper] for the symmetric part of the temperature distribution; see Appendix 1.} These authors used an eddy diffusivity ratio $\varepsilon_\phi/\varepsilon_r$ which was dependent upon radial position, Re and Pr, and which will be described more fully in the discussion of the results of the present investigation. With the data available to Gärtner, Johannsen and Ramm the comparison with experimental data was not conclusive.

It was decided that the present experimental investigation should employ a mass-transfer method, to avoid the problems of heat loss and conduction in the pipe wall, a concentric annulus being chosen because it provides an inherently more sensitive test of circumferential diffusion models as suggested earlier [6] and confirmed by preliminary design calculations.

FORMULATION OF EQUATIONS AND THEIR SOLUTION

We consider three-dimensional mass transfer in fully-developed turbulent flow between the two impermeable walls of a concentric annulus. The situation is depicted in Fig. 1.

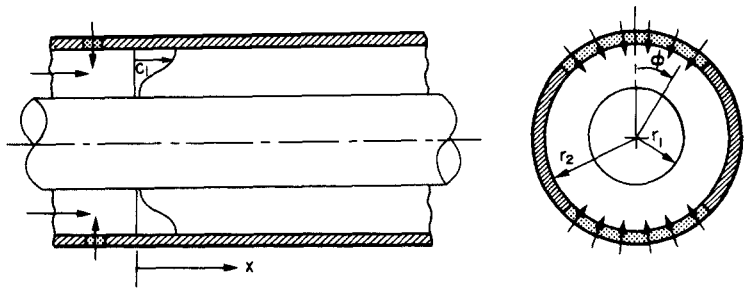

FIG. 1. Diagrammatic arrangement of the apparatus.

In non-dimensional form the differential equation for conservation of the diffusing species is

$$u_2^+ r_2^+ \frac{2(s-1)}{s}\frac{1}{ReSc}\frac{\partial\theta}{\partial x^+} = \frac{1}{\rho}\frac{\partial}{\partial\rho}\left[\rho\left(\frac{1}{Sc}+\frac{\varepsilon_{Mr}}{\nu}\right)\frac{\partial\theta}{\partial\rho}\right] + \frac{1}{\rho^2}\frac{\partial}{\partial\phi}\left[\left(\frac{1}{Sc}+\frac{\varepsilon_{M\phi}}{\nu}\right)\frac{\partial\theta}{\partial\phi}\right] \quad (1)$$

with boundary conditions

$$\frac{\partial\theta}{\partial\rho} = 0 \quad \text{at} \quad \rho = \rho_1 \quad \text{and} \quad \rho_2$$

and, taking the origin of x at the axial station where the initial concentration distribution is known,

$$\theta = \theta_i(\rho, \phi) \quad \text{at} \quad x^+ = 0.$$

By separating the variables the solution can be developed in the form

$$\theta(\rho, \phi, x^+) = 1 + \sum_{m=1}^{\infty} C_m R_{m0} \exp(-\beta_{m0}^2 x^+) + \sum_{n=1}^{\infty} A_n(\cos\gamma_n\phi + B_n \sin\gamma_n\phi) \times \sum_{m=1}^{\infty} K_{mn} R_{mn} \exp(-\beta_{mn}^2 x^+) \quad (2)$$

where the three terms on the RHS correspond to the fully-developed uniform concentration, the axisymmetric developing component and the non-axisymmetric developing component respectively. The eigenvalues, β_{mn}, and eigenfunctions, R_{mn}, are given by the solution of the Sturm–Liouville problem

$$\frac{1}{\rho}\frac{\mathrm{d}}{\mathrm{d}\rho}\left[\rho\left(\frac{1}{Sc}+\frac{\varepsilon_{M,r}}{\nu}\right)\frac{\mathrm{d}R}{\mathrm{d}\rho}\right] + \left[\frac{u_2^+ r_2^+}{ReSc}\frac{2(s-1)}{s}\beta^2 - \frac{\gamma_n^2}{\rho^2}\left(\frac{1}{Sc}+\frac{\varepsilon_{M\phi}}{\nu}\right)\right]R = 0 \quad (3)$$

with the impermeable wall boundary conditions

$$\frac{\mathrm{d}R}{\mathrm{d}\rho} = 0 \text{ at } \rho = \rho_1 \text{ and } \rho_2.$$

The present investigation was concerned with the situation depicted in Fig. 1 for which the circumferential concentration has a period π. Therefore, taking the origin of ϕ as shown,

$$B_n = 0 \quad \text{and} \quad \gamma_n = 2n.$$

In order to produce a solution in the form of equation (2) for the decay of an initial concentration distribution along an annular passage it is necessary to specify: (a) the velocity profile; (b) the eddy diffusivity of mass in the radial direction; (c) the eddy diffusivity of mass in the circumferential direction; and (d) to fit the solution to the initial distribution. The principal objective of this investigation was to obtain information on the magnitude of circumferential diffusion, (c) above, but the experiment was designed to provide evidence on (a) and (b) also. A brief description of the experimental design will be followed by reviews of the present experimental results for topics (a), (b) and (c) in turn.

EXPERIMENTAL DESIGN

The concentric annular test section, Fig. 1, had nominal inner and outer diameters of 70 and 140 mm. An air entry section providing a 16:1 contraction and containing a honeycomb was followed by a generous hydrodynamic entry length of 60 equivalent diameters. Then came the short nitrous oxide injection section, followed by the test section with a length of 45 equivalent diameters, then an orifice plate section and the fan, which discharged the nitrous oxide–air mixture outside the laboratory. The core was located by three sets of three radial struts, two sets being upstream and one set downstream of the mass-transfer test section. The struts were of aerofoil section and no disturbance to the velocity profile could be detected at entry to the test section. The struts were adjustable radially to locate the core centrally and the variation of the annular gap was everywhere well within $\pm 1\%$. Radial velocity distribution measurements confirmed that the flow at the test section was fully-developed, with a high degree of symmetry, and the flow rate obtained by integration of the velocity profile agreed within 1% with that from the orifice plate.

The nitrous oxide injection section consisted of a permeable graphite ring of 20 mm square cross-section, flush with the outer tube surface. Graphite was selected as having the most uniform permeability of the materials investigated. Nevertheless the injection rate proved to be far from uniform circumferentially but a satisfactory distribution was achieved by a trial and error process of blanking off parts of the surface with paint. The same method was used to obscure two

quadrants of the ring for the non-axisymmetric injection tests.

Twelve insertion points for pitot tubes or concentration sampling probes were equally-spaced, in-line, along the test section, and the outer pipe could be rotated relative to the adjacent sections to investigate the circumferential distribution. Nitrous oxide concentrations were all in the range 0–200 ppm and were measured by infra-red gas analyser. The process is slow so that a single radial traverse would take about 100 min. An automatic traversing system was therefore devised, with adjustable step-wise motion and dwell time, and there was automatic logging of position and concentration.

Full details of the apparatus and experimental procedures can be found in the thesis [12].

VELOCITY PROFILES

These were measured at four values of Re in the range 3.6 to 11.0×10^4 using a pitot tube of 0.35 mm diameter, with corrections for wall proximity, Macmillan [16], and for velocity gradient effects and turbulence, Kinghorn [17].

Shear stresses for each of the surfaces were required for the conversion of the measured velocity profiles into $u^+ - y^+$ coordinates for the inner and outer regions. The overall annulus friction factor data (seven points over the Re range $3.8–12.0 \times 10^4$) were well represented by $f = 0.0657 Re^{-0.225}$. This correlation, which falls in the middle of the scatter band of other empirical correlations for annuli, was used in all subsequent calculations. Shear stresses on the inner and outer surfaces were separated by estimating the radius of maximum velocity, which is known to be indistinguishable from the surface of zero shear at this radius ratio. Precise estimation of the maximum velocity position is difficult; the present estimates of r_m/r_1 tended to be at the upper end of the range of previous results, but not inconsistent with them.

Quarmby [18] has shown experimentally that the radius of maximum velocity is both Reynolds number and radius ratio dependent, and subsequently [19] he has developed a velocity profile calculation model that includes such dependence. With this model four zones are distinguished: a wall layer and a turbulent core for the inner and the outer regions. Deissler's [20] expression for the eddy diffusivity of momentum is adopted for the wall layers, which leads to

$$\frac{du_1^+}{dy_1^+} = \frac{\tau/\tau_1}{1 + n_1^2 u_1^+ y_1^+} [1 - \exp(-n_1^2 u_1^+ y_1^+)] \qquad (4)$$

for $0 < y_1^+ < y_{i1}^+$

with a similar expression for the outer region. For the turbulent cores von Karman's similarity hypothesis leads to

$$\frac{d^2 u_1^+}{dy_1^{+2}} = \frac{-K(du_1^+/dy_1^+)^2}{\left[\frac{\tau}{\tau_1} - \frac{du_1^+}{dy_1^+}\right]^{1/2}}, \quad y_{i1}^+ < y_1^+ < y_{m1}^+ \qquad (5)$$

and similarly for the outer region. The velocities and velocity gradients are matched at the edge of the sub-layer; like-wise the velocities at the junction of the two turbulent cores, a condition which determines the radius of maximum velocity. The calculated values of this radius were virtually identical to the experimental estimates at the lower Re and smaller to the extent of 1% of the annulus width at the upper Re.

The measured velocity profiles were compared with predictions using Quarmby's model and also with the law of the wall in the form:

$$u^+ = 5 \ln y^+ - 3.05 \quad 5 < y^+ < 30$$
$$u^+ = 2.5 \ln y^+ + 5.5 \quad y^+ > 30.$$

The law of the wall gave quite a good fit, rather better in the outer region than the inner one, but the Quarmby model was better. Moreover, other workers have shown that the Quarmby model satisfactorily describes the velocity distribution at high radius ratios where the law of the wall has proved inadequate, particularly in the inner region. Velocity profiles calculated by Quarmby's model were therefore used in the solution of the equation for the concentration distribution.

DIFFUSIVITY OF MASS IN THE RADIAL DIRECTION

In the differential equation for the concentration distribution [1] we now consider the factor

$$\left(\frac{1}{Sc} + \frac{\varepsilon_{M,r}}{\nu}\right) \quad \text{i.e.} \quad \left(\frac{1}{Sc} + \frac{\varepsilon_{m,r}}{\nu}\frac{1}{Sc_t}\right)$$

and we discuss, in turn, Sc, $\varepsilon_{m,r}$ and Sc_t.

The Schmidt number for dilute concentrations of nitrous oxide in air has been quoted, almost invariably, as 0.77. Both Anand [11] and Davis [21] quote this value at 20°C but there are surprising inconsistencies:

	Anand	Davis
ν	11.47	15.2
D	14.89	20

The units are 10^{-6} m^2/s. Davis's values for ν and D are one-third larger than Anand's. Davis's ν is close to established values; while for D, calculations from Chapman–Enskog theory give 14.76, in good agreement with Anand! On this basis the Schmidt number is 1.02. Spalding [22] gave an approximate expression for the Schmidt number for dilute mixtures in air: $Sc \simeq 0.145 M^{0.556}$, where M is the molecular weight of the tracer gas, from which $Sc = 1.19 \pm 20\%$ for nitrous oxide; this tolerance band contains 1.02 but not 0.77. Except very close to the wall the molecular diffusivity is small compared to the turbulent diffusivity; therefore a change in Sc from 0.77 to 1.02 is not significant for the present investigation but the discrepancy is worth recording.

The von Karman formulation for the velocity distribution in the turbulent core, equation (5), leads to a zero value for the eddy diffusivity of momentum at

the radius of maximum velocity. Although the velocity distribution is satisfactory, a zero eddy diffusivity is unacceptable for the mass diffusion problem. To resolve this difficulty we have used a diffusivity model having its origin in a proposal by Reichardt [23] for the circular tube geometry and which gives a non-zero eddy diffusivity at the maximum velocity position. This model was adapted to the turbulent core region of an annular geometry by Leung, Kays and Reynolds [24] and subsequently modified by Quarmby [25] to achieve continuity of eddy diffusivity with Deissler's model at the edge of the wall layer. If this eddy diffusivity model is used to calculate the velocity profile the agreement with experiment is not quite so good as with the von Karman formulation. Despite the slight inconsistency, the proposed velocity profile and eddy diffusivity formulations have been used successfully in combination by Quarmby [25, 26] for heat-transfer predictions for annuli, with a variety of thermal boundary conditions and embracing both thermal entry and fully-developed conditions.

There is considerable scatter among the theoretical models and experimental data for the turbulent Schmidt (or Prandtl) number. However, most of the models give a turbulent Schmidt number of unity when Sc is unity. Consequently since Sc is taken to be 1.02 in the present instance we can assume that Sc_t is unity.

Radial concentration profiles were measured, with axisymmetric injection of nitrous oxide, at 12 axial stations downstream of the porous injection section, and for four Re from 3.61 to 11.0 $\times 10^4$. The procedure then was to compare the observed decay of the concentration profiles with the predictions from

$$\theta(\rho, x^+) = 1 + \sum_{m=1}^{\infty} C_m R_{m0} \exp(-\beta_{m0}^2 x^+)$$

which is equation (2) after the non-axisymmetric terms have been discarded.

The eigenvalues, β_{m0}, and eigenfunctions, R_{m0}, were computed from the numerical solution of the Sturm–Liouville problem as described by equation (3) with $n = 0$. A fourth-order Runge–Kutta integration procedure was employed which made use of 600 increments in radius from the inner to the outer wall of the annulus. The procedure was shown to give a high degree of accuracy when compared with existing numerical solutions for laminar flow [27, 28] and also an analytical solution for laminar slug flow [12].

The coefficients C_m were obtained by fitting the series to the measured initial distribution. It was found that a large number of terms in the series, and an excessive computing time, would be required to represent adequately the first radial concentration profile, taken 4.64 equivalent diameters after the injection section. It was therefore decided to discard the profiles from the first four stations and to use as the initial profile the results from the station 14.6 equivalent diameters after the injection section; ten terms in the series gave an excellent fit to this measured initial profile, Fig. 2. Figure 3 shows, for the same test condition, a comparison of the measured and calculated concentration profiles at the station 38.2 equivalent diameters from the injection section. For the calculations using $Sc_t = 1.0$ the agreement is excellent, whereas use of $Sc_t = 1/1.2$ (as suggested by Kays and Leung [29]) is clearly less satisfactory. The agreement between the measured and calculated (with $Sc_t = 1.0$) profiles was found to be excellent for all axial stations and Reynolds numbers. The radial eddy diffusivity of mass was also obtained directly from the measured profiles by integrating the equation for conservation of species with respect to radius to give

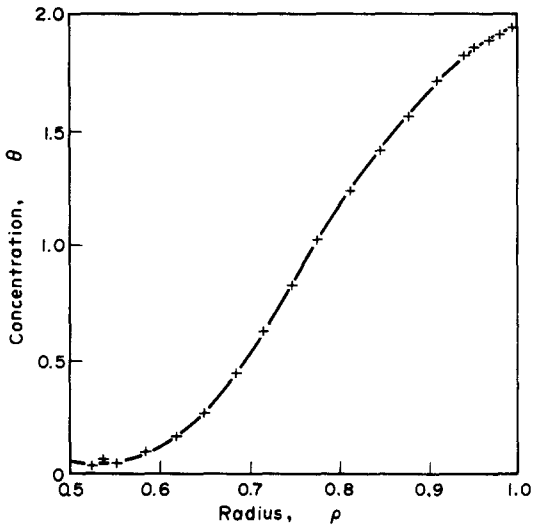

FIG. 2. Initial concentration profile—experimental points and series solution.

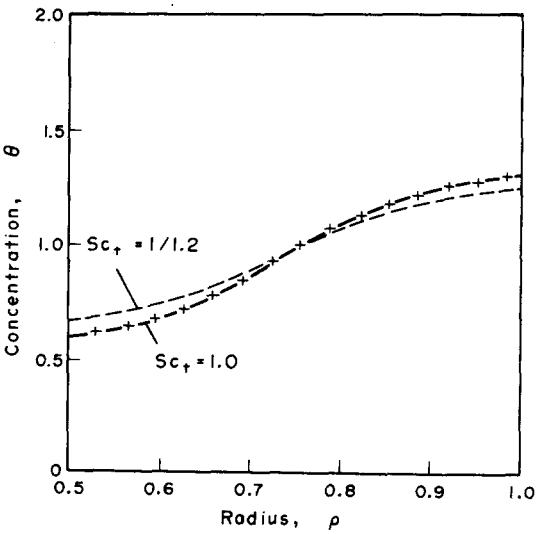

FIG. 3. Experimental concentration profile and calculated profiles for different turbulent Schmidt numbers, $Re = 1.10 \times 10^5$.

$$\frac{\varepsilon_{M,r}}{\nu} = \frac{\dfrac{r_2^+}{ReSc}\dfrac{2(s-1)}{s}\displaystyle\int_{\rho_1}^{\rho} \rho u_2^+ \frac{\partial\theta}{\partial x^+}\,d\rho}{\rho\dfrac{\partial\theta}{\partial\rho}} - \frac{1}{Sc}$$

for the inner region, with a similar expression for the outer region. This involved the determination of the

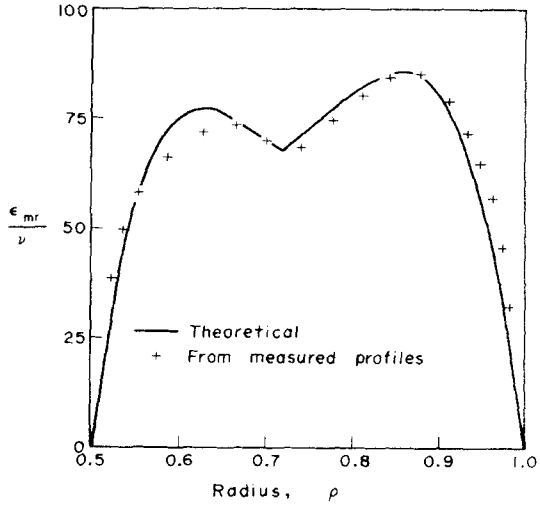

FIG. 4. Radial eddy diffusivity of mass, $Re = 7.28 \times 10^4$.

axial concentration gradient $\partial\theta/\partial x^+$ from the profiles at five consecutive axial stations, and the radial gradient $\partial\theta/\partial\rho$, the differentiation routine of Hennion [30] being used in both instances. A typical result is given in Fig. 4; the curve is the theoretical $\varepsilon_{m,r}/\nu$ which, with $Sc_t = 1.0$, is identical to $\varepsilon_{M,r}/\nu$. In view of the difficulty of differentiating the measured profiles accurately, the agreement is good and, together with the good agreement between the measured and calculated decaying concentration profiles, confirms the soundness of the radial diffusion model.

DIFFUSIVITY OF MASS IN THE CIRCUMFERENTIAL DIRECTION

To determine the eigenvalues, β_{mn}, and eigenfunctions, R_{mn}, for non-axisymmetric mass transfer ($n \geqslant 1$) we need to specify $\varepsilon_{M,\phi}$. Calculations have been made for five different formulations for $\varepsilon_{M,\phi}/\varepsilon_{M,r}$ starting with the simplest assumption that the ratio is unity at every point. Elder [31] studied the dispersion of permanganate solution dropped on to the surface of water flowing in a rectangular channel of large aspect ratio. The results were obtained at low Reynolds numbers but the tentative indications that the lateral diffusivity was substantially greater than the normal diffusivity have been introduced into the present calculations in the form $\varepsilon_{M,\phi}/\varepsilon_{M,r}$ equal to 3.0.

Turbulence measurements suggest that $\varepsilon_{M,\phi}/\varepsilon_{M,r}$ varies with radial position. The results of Laufer [32] for a circular tube show that w'/v' increases slowly with r from unity at the centre-line to 1.3 at $r/a = 0.8$ and then more rapidly as the wall is approached. The degree of anisotropy was found to increase with Reynolds number such that the maximum values of w'/v' were about 1.64 at $Re' = 5 \times 10^4$ and 2.24 at $Re' = 5 \times 10^5$. The results of Brighton [33] for an annulus showed a similar pattern of anisotropy, w'/v' being greater than unity everywhere except near the point of maximum velocity and rising to about 1.4 near the walls. The three remaining models used in the present calculations all included a radial variation of $\varepsilon_{M,\phi}/\varepsilon_{M,r}$.

The theoretical and experimental work of Bobkov *et al.* [34, 35] for circular tubes has been adapted to an annulus in the form

$$\frac{\varepsilon_{M,\phi}}{\varepsilon_{M,r}} = 1.0 + \frac{0.2}{1.02 - R}$$

where

$$R = \frac{r_m - r}{r_m - r_1} \quad \text{for} \quad r_1 < r \leqslant r_m$$

and

$$R = \frac{r - r_m}{r_2 - r_m} \quad \text{for} \quad r_m \leqslant r < r_2.$$

With this form the characteristics proposed by Bobkov *et al.* are preserved viz. $\varepsilon_{M,\phi}/\varepsilon_{M,r} = 1.2$ at the radius of maximum velocity, r_m, and tending to 11.0 at both surfaces.

Quarmby and Quirk [14] plotted $\varepsilon_{M,\phi}/\varepsilon_{M,r}$ against radial position in a circular tube based upon the analysis of heat- and mass-transfer experiments. The value of this ratio was found to be large near the wall but not substantially greater than unity over most of the cross-section. No systematic effect of Reynolds number could be discerned. A mean curve through their experimental data has been used in the present calculations after being adapted to an annulus as explained above for the Bobkov model.

Gärtner, Johannsen and Ramm have discussed both radial and circumferential diffusivities in a series of theoretical papers [15, 36, 37, 38]. A detailed description of their method does not appear to have been published but it is evidently based upon the ideas of Buleev. Their principal modification of Buleev's approach was to permit length scales occurring in the definitions of the diffusivities to be made dependent upon direction and related to the geometry of the duct cross-section; in addition, for duct shapes in which secondary flow would be expected to occur its effects were simulated by artificially increasing the anisotropy of the eddy diffusivity.

The results for annuli [38] are that: "The ratio $\varepsilon_{h\phi}/\varepsilon_{hr}$ varies across the flow section having a sharp maximum in the region close to the wall. As Re increases the value of the maximum rises rapidly and its location approaches the wall. For reasons of symmetry, the $\varepsilon_{h\phi}/\varepsilon_{hr}$ profiles at the inner and outer walls are equal for $r_1/r_2 = 1.0$. As r_1/r_2 decreases, the ratio increases in the inner portion of the annulus and diminishes in the outer portion. With respect to Pr it was found that its effect is insignificant". The scope of the last statement is not clear as the title of the paper specifies liquid metals and all results shown are for Pr of 0.025. Moreover, a later paper [15], dealing with circular pipes, indicates that $\varepsilon_{h\phi}/\varepsilon_{hr}$ is significantly greater for gases than for liquid metals. Ramm and Johannsen [38] include plots of $\varepsilon_{h\phi}/\varepsilon_{hr}$ for the inner and outer regions of an annulus with $r_2/r_1 = 2$ as used in the present investigation. The curves are for Re of 4.5×10^4, which lies within the Re range of the present investigation. For a plain circular tube, the effect of

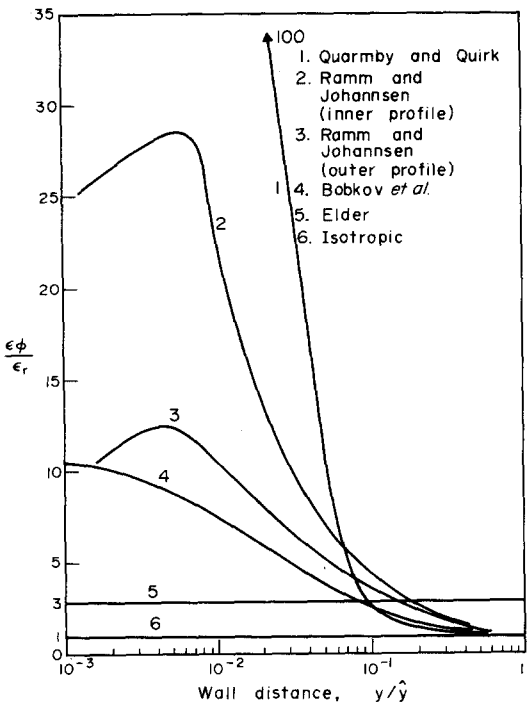

FIG. 5. Circumferential eddy diffusivity models.

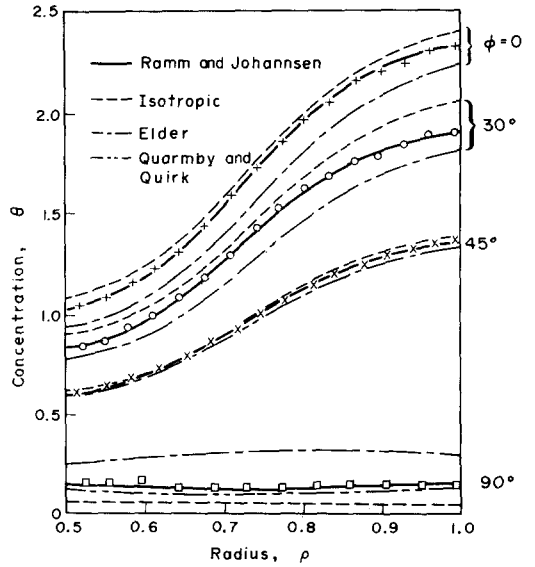

FIG. 6. Comparison of experimental and theoretical concentration profiles, $Re = 1.09 \times 10^5$, $x/d_e = 31$. —— Ramm and Johannsen; --- isotropic; ——— Elder; ——— Quarmby and Quirk.

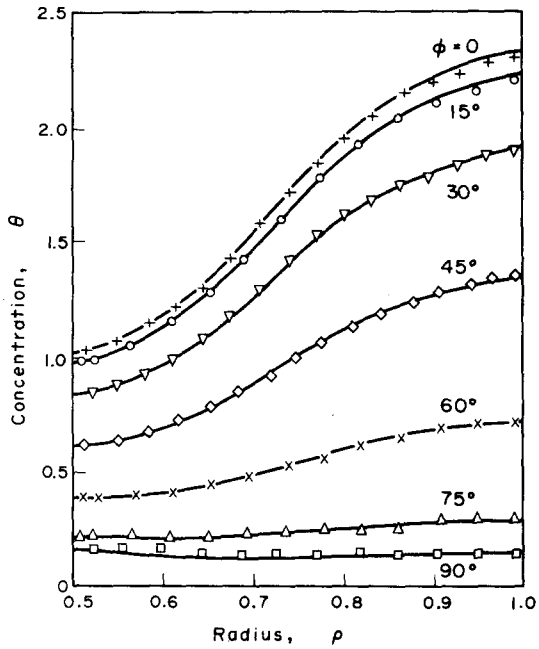

FIG. 7. Comparison of experimental and theoretical concentration profiles, Ramm and Johannsen model, $Re = 1.09 \times 10^5$, $x/d_e = 31$.

increasing Re, presented in the same paper, is to increase $\varepsilon_{h\phi}/\varepsilon_{hr}$ in the wall region. However, in the absence of such information for the annulus, the curves for $r_2/r_1 = 2$ have been used without variation for Re in the present calculations.

Figure 5 illustrates the five different formulations for $\varepsilon_{M,\phi}/\varepsilon_{M,r}$ used in the calculations of eigenvalues and eigenfunctions.

With nitrous oxide injection from two quadrants, Fig. 1, radial concentration profiles were measured at 12 axial stations for angular locations of 0, 15, 30, 45, 60, 75 and 90° and two Reynolds numbers, 3.6 and 10.9 $\times 10^4$. Subsequently it was found that the distribution at the third axial station could be fitted accurately using the terms $m = 1$–7 and $n = 1$–7 in the double series, equation (2). The measured decay of the distribution over a further 31 equivalent diameters was then compared with predictions based on the different circumferential diffusion models.

The greatest differences between the predictions were shown to exist at the most downstream station. Figure 6 shows a comparison between the measurements and the solutions for the isotropic, Elder, Quarmby and Quirk, and Ramm and Johannsen models. The calculations based upon Bobkov are indistinguishable from Quarmby and Quirk, and only at 90° is the latter significantly different from Ramm and Johannsen. The fact that these models differ substantially in the immediate wall region is not significant for these calculations. The Ramm and Johannsen model was found to give an excellent fit to the measurements at the other angular positions. Fig. 7, at the intermediate axial stations, and at the lower Re, Fig. 8. The excellent fit at both Re, notwithstanding that the Re dependence of $\varepsilon_{M,\phi}/\varepsilon_{M,r}$ has not been included, again signifies that the present comparisons are not sensitive to the immediate wall region where the principal Re dependence is believed to be located.

CONCLUDING REMARKS

The first part of this investigation has confirmed the soundness of the velocity profile and the radial diffusion model, provided that the turbulent Schmidt number is taken as unity for the diffusion of nitrous oxide in air. The results for non-axisymmetric nitrous

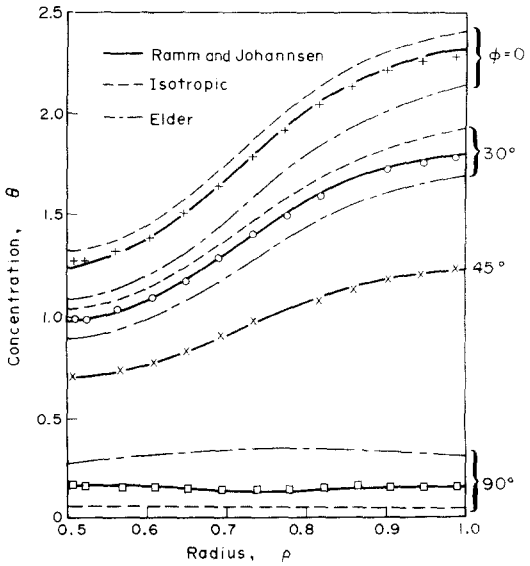

FIG. 8. Comparison of experimental and theoretical concentration profiles, $Re = 3.60 \times 10^4$, $x/d_e = 31$. —— Ramm and Johannsen; – – – isotropic; — — — Elder.

oxide injection confirm the expectation that the annular geometry, given sufficient experimental care, is capable of greater discrimination between different circumferential diffusion models than has been achieved hitherto. The isotropic assumption, $\varepsilon_{M\phi}/\varepsilon_{Mr} = 1.0$, underestimates the circumferential diffusion, while $\varepsilon_{M\phi}/\varepsilon_{Mr} = 3.0$, prompted by Elder's results, overestimates it. The Ramm and Johannsen model, in which $\varepsilon_{M\phi}/\varepsilon_{Mr}$ varies with radial position, provides an excellent fit to all the experimental data. The Bobkov and Quarmby and Quirk formulations fit the experimental results quite well despite the fact that they differ from each other and from Ramm and Johannsen markedly in the wall region. Evidently the present results are incapable of discriminating between different levels of $\varepsilon_{M\phi}/\varepsilon_{Mr}$ close to the wall or of confirming the Reynolds number dependence of $\varepsilon_{M\phi}/\varepsilon_{Mr}$ in the wall region proposed by Ramm and Johannsen. Indeed it could be that a constant value of $\varepsilon_{M\phi}/\varepsilon_{Mr}$ of about 2.0 would fit the present experimental results tolerably well. However, there is support from turbulence measurements for formulations in which the degree of anisotropy varies with radial position and is substantial only in the wall region.

The scope for further work along the same lines to define more closely the radial variation of $\varepsilon_{M\phi}/\varepsilon_{Mr}$ could include the calculation of higher eigenvalues and eigenfunctions for comparison with concentration distribution measurements closer to the source; the provision of a source in the inner surface in addition to the outer one; and an extension to different radius ratios.

REFERENCES

1. W. C. Reynolds, Turbulent heat transfer in a circular tube with variable circumferential heat flux, *Int. J. Heat Mass Transfer* **6**, 445–454 (1963).
2. R. D. Cess, A survey of the literature on heat transfer in turbulent tube flow, University of Pittsburg, Pennsylvania (1958).
3. R. Jenkins, Variation of the eddy conductivity with Prandtl modulus and its use in prediction of turbulent heat transfer coefficients, Heat Transfer and Fluid Mechanics Institute, Stanford University Press, Stanford, California (1955).
4. W. C. Reynolds, Effect of wall heat conduction on convection in a circular tube with arbitrary circumferential heat input, *Int. J. Heat Mass Transfer* **6**, 925 (1963).
5. E. M. Sparrow and S. H. Lin, Turbulent heat transfer in a tube with circumferentially-varying temperature or heat flux, *Int. J. Heat Mass Transfer* **6**, 866–867 (1963).
6. W. A. Sutherland and W. M. Kays, Heat transfer in an annulus with variable circumferential heat flux, *Int. J. Heat Mass Transfer* **7**, 1187–1194 (1964).
7. A. W. Black and E. M. Sparrow, Experiments on turbulent heat transfer in a tube with circumferentially varying thermal boundary conditions. *J. Heat Transfer* **89**, 258–268 (1967).
8. A. C. Rapier, Forced convection heat transfer in a circular tube with non-uniform heat flux around the circumference, *Int. J. Heat Mass Transfer* **15**, 527–537 (1972).
9. A. Quarmby and R. K. Anand, Non-axisymmetric turbulent mass transfer in a circular tube. *J. Fluid Mech.* **38**, 457–472 (1969).
10. A. Quarmby and R. K. Anand, Axisymmetric turbulent mass transfer in a circular tube. *J. Fluid Mech.* **38**, 433–455 (1969).
11. R. K. Anand, Mass transfer in non-axisymmetric situations in turbulent flow in a circular tube, Ph.D. Thesis, University of Manchester Institute of Science and Technology (1968).
12. D. P. Robinson, Anisotropic turbulent mass transfer in an annulus, Ph.D. Thesis, University of Bradford (1975).
13. A. Quarmby, Calculations of the effect of tangential eddy diffusivity on non-symmetric turbulent diffusion in a plain tube, *Int. J. Heat Mass Transfer* **15**, 866–870 (1972).
14. A. Quarmby and R. Quirk, Measurements of the radial and tangential eddy diffusivities of heat and mass in turbulent flow in a plain tube, *Int. J. Heat Mass Transfer* **15**, 2309–2327 (1972).
15. D. Gärtner, K. Johannsen and H. Ramm, Turbulent heat transfer in a circular tube with circumferentially varying thermal boundary conditions, *Int. J. Heat Mass Transfer* **17**, 1003–1018 (1974).
16. F. A. Macmillan, Experiments on pitot tubes in shear flow, Ministry of Supply, R and M No. 3028 (1956).
17. F. C. Kinghorn, The effects of turbulence and transverse velocity gradients on pitot-tube observations, NEL Report No. 464 (1970).
18. A. Quarmby, An experimental study of turbulent flow through concentric annuli, *Int. J. Mech. Sci.* **9**, 205–221 (1967).
19. A. Quarmby, An analysis of turbulent flow in concentric annuli, *Appl. Scient. Res.* **19**, 250–273 (1968).
20. R. G. Deissler, Analysis of turbulent heat and mass transfer in smooth tubes at high Prandtl and Schmidt number, NACA Rep. 1210 (1953).
21. J. T. Davis, *Turbulence Phenomena*. Academic Press, New York (1972).
22. D. B. Spalding, *Convective Mass Transfer*. Edward Arnold, London (1963).
23. H. Reichardt, Complete representation of turbulent velocity in a smooth pipe, *Z. Angew. Math. Mech.* **31**, 208 (1951).
24. E. Y. Leung, W. M. Kays and W. C. Reynolds, Heat transfer with turbulent flow in concentric and eccentric annuli with constant and variable heat flux, Report AHT-4, Dept. of Mech. Engng, Stanford University, California (1962).
25. A. Quarmby, Fully developed turbulent heat transfer in a concentric annulus with uniform wall heat fluxes, *Chem. Engng Sci.* **24**, 171–187 (1969).

26. A. Quarmby and R. K. Anand, Turbulent heat transfer in concentric annuli with constant wall temperatures, *J. Heat Transfer* **92**, 33–45 (1970).
27. A. P. Hatton and A. Quarmby, Heat transfer in the thermal entrance region with laminar flow in an annulus, *Int. J. Heat Mass Transfer* **5**, 973–980 (1962).
28. R. E. Lundberg, W. C. Reynolds and W. M. Kays, Heat transfer with laminar flow in concentric annuli with constant and variable wall temperature and heat flux, NASA TN D-1972 (1963).
29. W. M. Kays and E. Y. Leung, Heat transfer in annular passages—hydrodynamically developed turbulent flow with arbitrarily prescribed heat flux, *Int. J. Heat Mass Transfer* **6**, 537–557 (1963).
30. P. E. Hennion, Algorithm 77—Interpolation, differentiation and integration, *Communs Ass. Comput. Mach.* **5**, 96 (1962).
31. J. W. Elder, The dispersion of marked fluid in turbulent shear flow, *J. Fluid Mech.* **5**, 544–560 (1959).
32. J. Laufer, The structure of turbulence in fully developed pipe flow, NACA Report 1174 (1952).
33. J. A. Brighton, The structure of fully-developed turbulent flow in annuli, Ph.D. Thesis, Purdue University (1963).
34. V. P. Bobkov, M. Kh. Ibraginiov and V. I. Subbotin, Calculating the coefficient of turbulent heat transfer for a liquid flowing in a tube, *Atom. Energy (USSR)* **24**, 545–560 (1968).
35. V. P. Bobkov, M. Kh. Ibraginiov and G. I. Sabelov, The calculation of turbulent heat diffusion in channels of non-circular cross section, *High Temperature* **6**, 645–651 (1968).
36. H. Ramm and K. Johannsen, Hydrodynamics and heat transfer in regular arrays of circular tubes, in 1972 *International Seminar on Recent Developments in Heat Exchangers*, Trogir, Yugoslavia (1972).
37. K. Johannsen and H. Ramm, Note on tangential eddy diffusivity in a circular tube, *Int. J. Heat Mass Transfer* **16**, 1803–1805 (1973).
38. H. Ramm and K. Johannsen, Radial and tangential turbulent diffusivities of heat and momentum transfer in liquid metals, in *Progress in Heat and Mass Transfer*, Vol. 7, pp. 45–58. Pergamon Press, Oxford (1973).

APPENDIX

Pipe centre-line boundary conditions on the diffusion equation

The solution for the concentration distribution must satisfy two conditions at the centre-line of a pipe:

(i) the concentration must be single-valued;

(ii) the concentration gradients must be consistent with the absence of a source or sink of the diffusing substance along the centre-line, i.e.

$$\lim_{r\to 0} r\int_0^{2\pi}\frac{\partial c}{\partial r}\,\mathrm{d}\phi = 0.$$

The solution is normally separated into a symmetric and a non-symmetric part. Consider these in turn:

(a) Since ϕ does not appear in the symmetric part, (i) is satisfied automatically. Condition (ii) is then satisfied by imposing $\mathrm{d}R/\mathrm{d}r = 0$ at $r = 0$ on all the eigenfunctions involved in the symmetric part of the distribution. Gärtner, Johannsen and Ramm [15] made the mistake of using $R = 0$ at $r = 0$.

(b) The non-symmetric part involves a series of terms of the type $R_{mn}\cos 2n\phi$. In this case (ii) is satisfied automatically; (i) by imposing $R_{mn} = 0$ at $r = 0$ on each radial eigenfunction. Quarmby and Anand [9] made the mistake of using $\mathrm{d}R_{mn}/\mathrm{d}r = 0$ at $r = 0$; in consequence $R_{mn} \neq 0$ at $r = 0$ for the eigenfunctions quoted by Anand [11] and the calculated distribution is not single-valued at the centre-line.

Failures to satisfy checks for internal consistency of some of the numerical results quoted by Anand are discussed in [12].

CONVECTION MASSIQUE TURBULENTE DANS UN ESPACE ANNULAIRE AVEC DES CONDITIONS AUX LIMITES A DISSYMETRIE AXIALE

Résumé—Le principal objet de cette étude est de déterminer la diffusion circonférentielle résultant de conditions aux limites sans symétrie axiale, liées à des passages symétriques pour des écoulements secondaires. L'espace annulaire est choisi car il constitue un test plus sensible que le tube circulaire à cause du parcours circonférentiel de diffusion relativement plus grand; on a préféré le transfert de masse parce qu'il évite les problèmes de pertes thermiques et de conduction thermique dans les parois du tube. L'oxyde d'azote est introduit dans l'air en écoulement à travers des régions poreuses dans la paroi externe et les distributions de concentration mesurées en aval sont comparées avec les solutions théoriques. Par des mesures préliminaires sont déterminés les profils de vitesse et la formulation de la diffusivité turbulente massique radiale en utilisant une source axisymétrique d'oxyde d'azote. Des distributions de concentration expérimentales pour l'injection sans symétrie axiale sont comparées avec des calculs basés sur plusieurs formulations du rapport des diffusivités $\varepsilon_{M,\phi}/\varepsilon_{M,r}$. L'hypothèse d'isotropie sous-estime la diffusion circonférentielle. Un excellent ajustement à toutes les mesures est obtenu avec un modèle dû à Ramm et Johannsen dans lequel le rapport $\varepsilon_{M,\phi}/\varepsilon_{M,r}$ varie avec la position radiale et croît fortement à l'approche des parois.

STOFFÜBERTRAGUNG BEI TURBULENTER STRÖMUNG IN EINEM RINGRAUM UND BEI NICHT-ACHSENSYMMETRISCHEN RANDBEDINGUNGEN

Zusammenfassung—Das Hauptziel dieser Untersuchung war es, die Größenordnung der Diffusion in Umfangsrichtung zu bestimmen, die sich bei nicht-achsensymmetrischen Randbedingungen und ohne Sekundär-strömungen in symmetrischen Spa'ten ergibt. Es wurde ein konzentrischer Ringraum gewählt, denn mit seinem relativ langen Diffusionsweg in Umfangsrichtung bietet er eine empfindlichere Versuchsanordnung für Diffusionsmodelle als ein Kreisrohr. Eine Stoffübertragungsmethode wurde gewählt, weil diese die Probleme der Wärmeverluste und der Wärmeleitung in den Rohrwänden vermeidet. Stickstoffoxydul wurde durch poröse Abschnitte der äußeren Wand in den Luftstrom eingebracht und die strömungsabwärts gemessene Konzentrationsverteilung wurde mit theoretischen Lösungen verglichen. Vorbereitende Messungen wurden zur Überprüfung des Geschwindigkeitsprofils—unter Verwendung einer achsensym-

metrischen Stickstoffoxydul-Quelle—und des Ansatzes für die radiale turbulente Diffusionskonstante gemacht. Anschließend wurden gemessene Konzentrationsverteilungen, die sich bei nichtachensymmetrischer Einführung ergeben, mit Vorhersagen für verschiedene Verhältnisse der Diffusionszahlen $\varepsilon_{M,\phi}/\varepsilon_{M,r}$ verglichen. Bei der Annahme von Isotropie ergibt sich eine zu geringe Diffusion in Umfangsrichtung. Eine ausgezeichnete Übereinstimmung mit allen Versuchsdaten wurde mit einem Modell nach Ramm und Johannsen erzielt, bei welchem sich das Verhältnis $\varepsilon_{M,\phi}/\varepsilon_{M,r}$ mit radialer Position ändert und merklich zunimmt, wenn man sich den Wänden nähert.

ПЕРЕНОС МАССЫ ПРИ ТУРБУЛЕНТНОМ ТЕЧЕНИИ В КОЛЬЦЕВОМ КАНАЛЕ С НЕОСЕСИММЕТРИЧНЫМИ ГРАНИЧНЫМИ УСЛОВИЯМИ

Аннотация — Основной целью данного исследования было определение тангенциального распределения диффузии, обусловленной неосесимметричностью граничных условий в симметричных каналах, в которых отсутствуют вторичные течения. Концентрический кольцевой канал выбран, исходя из того, что при характерной для него относительно большой длине, на которой происходит процесс диффузии, в нем можно проводить более точные, чем в круглой трубе, проверки диффузионных моделей. Выбор диффузионного метода объясняется тем, что он свободен от потерь тепла в стенках канала. Закись азота вводилась в поток воздуха через пористые вставки в наружной стенке канала. Полученные данные по распределению концентрации по потоку сравнивались с результатами численных расчётов. Были проведены предварительные измерения для проверки правильности расчёта профиля скорости и определения коэффициента турбулентной диффузии. Полученные экспериментальные значения распределения концентрации при неосесимметричной подаче закиси азота сравнивались с результатами расчётов для нескольких вариантов аппроксимации отношения коэффициентов диффузии $\varepsilon_{M,\phi}/\varepsilon_{M,r}$. В предположении изотропности найдено распределение величины диффузии по окружности. Получено хорошее соответствие всех экспериментальных данных с моделью Рамма и Ёсаннсена, в которой отношение $\varepsilon_{M,\phi}/\varepsilon_{M,r}$ изменяется в радиальном направлении, существенно возрастая по мере приближения к стенке канала.